

Ion Beam Studies of the Reactions of Group 8 Metal Ions with Alkanes. Correlation of Thermochemical Properties and Reactivity[†]

L. F. Halle, P. B. Armentrout, and J. L. Beauchamp*

Arthur Amos Noyes Laboratory of Chemical Physics, California Institute of Technology,
Pasadena, California 91125

Received December 14, 1981

With use of an ion beam apparatus, the gas-phase reactions of singly charged atomic iron and nickel ions with several alkanes are studied as a function of relative kinetic energy. Only endothermic processes are observed in the interactions of Fe⁺ and Ni⁺ with methane and ethane. Analysis of the thresholds for formation of the metal methyl ions from the reactions with ethane yields the bond dissociation energies $D^0(\text{Fe}^+-\text{CH}_3) = 69 \pm 5$ kcal/mol and $D^0(\text{Ni}^+-\text{CH}_3) = 48 \pm 5$ kcal/mol to be compared with the previously determined value $D^0(\text{Co}^+-\text{CH}_3) = 61 \pm 4$ kcal/mol. Exothermic carbon-carbon bond cleavage reactions are observed with all alkanes containing three or more carbon atoms. A mechanism involving oxidative addition of C-C and C-H bonds to the metal ions as a first step accounts for all products observed at all energies in this study. Differences in reactivity appear to be related to differences in metal-hydrogen and metal-carbon bond dissociation energies for the three group 8 metal ions.

Introduction

Transition metal alkyls appear as intermediates in many catalytic reactions.¹ Despite the importance of such information, the thermodynamics of the metal-organic fragment bonds is poorly known. Techniques which have been used to obtain this information include calorimetric² and kinetic studies in solution,³ mass spectrometric investigations,⁴ and ion cyclotron resonance mass spectrometry.⁵⁻⁷ In addition, calculations have also yielded energies for several metal-alkyl fragment bonds.⁸ More recently we have developed ion beam techniques for examining organometallic reactions in the gas phase.⁹⁻¹² In the present study, the ion beam apparatus is used to analyze the reactions of iron and nickel ions over a range of energies with various hydrocarbons. Bond energies are derived from an examination of the thresholds for the endothermic reactions using theoretical techniques which have been described in a previous paper.⁹ A detailed analysis of the reactions of the metal ions with ethane determines the metal ion-methyl bond energy. These data, combined with the bond strengths of metal ion-hydrogen bonds,^{10b,11} are used to interpret reactions with larger alkanes, with particular emphasis on the mechanism by which the metal ion cleaves carbon-carbon bonds. Results of the present study are compared and contrasted with earlier studies of the reactions of Co⁺ with alkanes,¹² hereafter referred to as I.

Experimental Section

The ion beam apparatus has been described in detail previously.⁹ Ions from a surface ionization source are accelerated and focused into a 60° sector magnet for mass separation. The mass selected beam is decelerated to the desired energy and focused into a collision chamber containing the reactant gas. Product ions scattered in the forward direction are focused into a quadrupole mass filter and detected by using a channeltron electron multiplier operated in a pulse-counting mode. Ion signal intensities are corrected for the mass discrimination of the quadrupole mass filter.

The ion source, previously described,¹⁰ is comprised of a tubular stainless-steel oven attached to the side of a U-shaped repeller plate which surrounds a rhenium ionization filament. The oven is loaded with FeCl₃ or NiCl₂·6H₂O. A rhenium filament generates sufficient heat to dehydrate and vaporize either complex. The metal chloride vapor is directed at the filament where it dissociates

and the resulting metal atom is ionized. At the filament temperature used, ~2400 K, it is estimated that over 98% of the nickel ions produced are in the (3d)⁹ ground-state configuration (²D), while less than 2% have the first excited-state configuration, (4s)(3d)⁸ (⁴F) which lies 1.04 eV above the ground state.¹³ At this same temperature, 77% of the iron ions are in their ³D ground-state manifold, with 22% in the first excited state (⁴F) which lies 0.232 eV above the ground state.¹³ Attenuation experiments¹⁴ indicate a single component in both beams, suggesting excited states are absent. However, this assumes that different states have substantially different cross sections for interaction with the attenuating gases (Ar, CH₄, N₂O).

The nominal collision energy of the ion beam is taken as the difference in potential between the collision chamber and the center of the filament, the latter being determined by a resistive divider. This energy is verified by use of a retarding field energy analyzer. Agreement was always within 0.3 eV. The energy distribution of the metal ion beams was also obtained by using

-
- (1) (a) Davidson, P. J.; Lappert, M. F.; Pearce, R. *Chem. Rev.* **1976**, *76*, 219. (b) Schrock, R. R.; Parshall, G. W. *Ibid.* **1976**, *76*, 243. (c) Halpern, J. *Trans. Am. Crystallogr. Assoc.* **1978**, *14*, 59.
 (2) (a) Adedeji, F. A.; Connor, J. A.; Skinner, H. A.; Galyer, L.; Wilkinson, G. *J. Chem. Soc., Chem. Commun.* **1976**, 159. (b) Lappert, M. F.; Patil, D. S.; Pedley, J. B. *Ibid.* **1975**, 830. (c) Calado, J. C. G.; Dias, A. R.; Martinho Simões, J. A. *Ibid.* **1978**, 737.
 (3) Halpern, J.; Ng, F. T. T.; Rempel, G. L. *J. Am. Chem. Soc.* **1979**, *101*, 7124.
 (4) Herberich, G. E.; Muller, J. *J. Organomet. Chem.* **1969**, *16*, 111.
 (5) Stevens, A. E.; Beauchamp, J. L. *J. Am. Chem. Soc.* **1978**, *100*, 2584; **1979**, *101*, 245.
 (6) (a) Allison, J.; Freas, R. B.; Ridge, D. P. *J. Am. Chem. Soc.* **1979**, *101*, 1332. (b) Allison, J.; Ridge, D. P. *Ibid.* **1979**, *101*, 4998. (c) Freas, R. B.; Ridge, D. P. *Ibid.* **1980**, *102*, 7129.
 (7) (a) Cody, R. B.; Burnier, R. C.; Reents, W. D., Jr.; Carlin, T. J.; McCrery, D. A.; Lengel, R. K.; Freiser, B. S. *Int. J. Mass Spectrom. Ion Phys.* **1980**, *33*, 37. (b) Burnier, R. C.; Byrd, G. D.; Frieser, B. S. *J. Am. Chem. Soc.* **1981**, *103*, 4360.
 (8) (a) Rappe, A. K.; Goddard, W. A., III *J. Am. Chem. Soc.* **1976**, *99*, 3966. (b) Sollenberger, M. J. M. S. Thesis, California Institute of Technology, 1976. (c) Walch, S. P.; Goddard, W. A., III *J. Am. Chem. Soc.* **1978**, *100*, 1338.
 (9) Armentrout, P. B.; Beauchamp, J. L. *J. Chem. Phys.* **1981**, *74*, 2819.
 (10) (a) Armentrout, P. B.; Beauchamp, J. L. *Chem. Phys.* **1980**, *48*, 315. (b) Armentrout, P. B.; Beauchamp, J. L. *Ibid.* **1980**, *50*, 37.
 (11) Armentrout, P. B.; Halle, L. F.; Beauchamp, J. L. *J. Am. Chem. Soc.* **1981**, *103*, 6501.
 (12) Armentrout, P. B.; Beauchamp, J. L. *J. Am. Chem. Soc.* **1981**, *103*, 784.
 (13) Moore, C. E. "Atomic Energy Levels"; National Bureau of Standards: Washington, D.C., 1949.
 (14) Turner, R. B.; Rutherford, J. A.; Compton, D. M. *J. J. Chem. Phys.* **1968**, *48*, 1602.

[†]Contribution No. 6564.

the retarding grid and was determined to be 0.7 eV (fwhm). In the center of mass frame, this introduces an uncertainty of less than ± 0.12 eV for the reactions with ethane. No specific account of the energy distribution of the ion beam is taken in the treatment below.

A more severe problem concerning the actual energy of interaction is the effect of the thermal motion of the reactant gas. Chantry¹⁵ has shown that the distribution of the relative kinetic energy at an energy E due to this effect has a full width at half-maximum of

$$W_{1/2} = (11.1\gamma kTE)^{1/2} \quad (1)$$

where T is the temperature of the target gas, 300 K, and $\gamma = m/(m + M)$, m and M being the masses of the incident particle and target gas. This energy distribution effectively broadens any sharp features in the excitation function, including the threshold. To account for this effect, the assumed excitation function is convoluted with this distribution before comparison with the data using the method outlined by Chantry.¹⁵

Reaction cross sections for a specific product, σ_i , are calculated from

$$\sigma_i = \sigma I_i / \sum I_i \quad (2)$$

where the sum is over all products and I_i refers to a particular measured product ion intensity. The total reaction cross section, σ , is evaluated by using

$$I_0 = (I_0 + \sum I_i) \exp(-n\sigma l) \quad (3)$$

where I_0 is the transmitted reactant ion beam intensity, n is the number density of the target gas, and l is the length of the interaction region. The pressure of the target gas, measured by using an MKS Baratron Model 90H1 capacitance manometer, is kept sufficiently low, $(1-5) \times 10^{-3}$ torr, that attenuation of the ion beam is minimal. The length of the interaction region is 5 mm. The experimental procedure employed involves taking a complete scan of kinetic energy at a single pressure to obtain the excitation function. At several energies, the product yield is measured as a function of pressure to ensure eq 2 and 3 are obeyed. This procedure also readily identifies products formed by more than one collision event.¹⁶

The greatest uncertainty in measurements of reaction cross sections is the ion detection efficiency. In experiments which involve heavy projectile and light target species, efficient detection is assisted by the appreciable center of mass velocity which tends to scatter all products in the forward direction in the laboratory frame. At laboratory energies below about 10 eV, a small field of 0.5 V is placed across the specially designed collision chamber¹⁷ to extract low energy ions. This field introduces an additional uncertainty in the energy of interaction. Relative cross sections are well reproduced, and we estimated that the absolute cross sections reported are accurate to within a factor of 2.

In the reaction of the metal ions with ethane the functional form for the energy dependent cross section, given by eq 4 is used

$$\begin{aligned} \sigma &= 0 & E \leq E_0 \\ \sigma &= \sigma_0 \left(\frac{E - E_0}{E} \right)^n & E_0 < E < E_0 + D/a \\ \sigma &= \sigma_0 \left(\frac{D}{aE} \right)^n & E \geq E_0 + D/a \end{aligned} \quad (4)$$

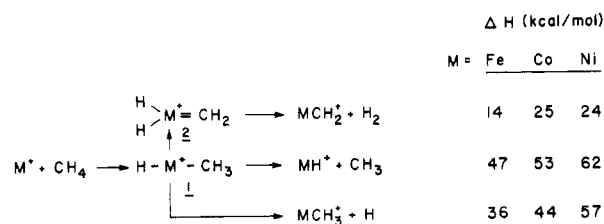
to fit the observed data and extract a bond dissociation energy.⁹ In eq 4 E is the total energy of the reactants and E_0 is the endothermicity of the reaction, taken to be the difference between the bond energy of the ionic product, D , and the bond energy of the neutral reactant. The average fraction of the total energy available to the products which is retained as internal excitation in the ionic fragment is given by a , and n is a variable exponent.

(15) Chantry, P. J. *J. Chem. Phys.* 1971, 55, 2746.

(16) Szabo, I. *Int. J. Mass Spectrom. Ion Phys.* 1969, 3, 169.

(17) Armentrout, P. B.; Hodges, R. V.; Beauchamp, J. L. *J. Chem. Phys.* 1977, 66, 4683.

Scheme I

Table I. Thermochemical Data^a

| bond energies | Fe ⁺ (3d) ⁶ (4s) (⁶ D) ^f | Co ⁺ (3d) ⁸ (³ F) ^f | Ni ⁺ (3d) ⁹ (³ D) ^f |
|--|---|--|--|
| $D^0(\text{M}^+ - \text{H})$ | 58 ± 5^b | 52 ± 4^c | 43 ± 2^d |
| $D^0(\text{M}^+ - \text{CH}_3)$ | 69 ± 5^e | 61 ± 4^c | 48 ± 5^e |
| $D^0(\text{M}^+ - \text{CH}_2)$ | 96 ± 5^b | 85 ± 7^f | 86 ± 6^b |
| $D^0(\text{M}^+ - \text{H}) + D^0(\text{M}^+ - \text{CH}_3)$ | 127 | 113 | 91 |
| $2D^0(\text{M}^+ - \text{H})$ | 116 | 104 | 86 |
| $2D^0(\text{M}^+ - \text{CH}_3)$ | 138 | 122 | 96 |

^a All values in kcal/mol. ^b Reference 11. ^c Reference 12. ^d Reference 10b. ^e This work. ^f Reference 9. ^g Ground state.

For the line of centers model,¹⁸ n is unity. If the reaction involves a polyatomic intermediate, n may be a sizable fraction of the total number of vibrational degrees of freedom. The cross section described by eq 4 is convoluted by using the method of Chantry¹⁵ to account for the thermal motion of the reactant gas as discussed above. Often, within experimental error, several sets of parameters fit the data equally well and thus give a range of possible threshold energies. It is in fact this analysis which gives the major uncertainty in E_0 .

It is important to point out that in these experiments neutral products are not detected. However, except at higher energies, the identity of these products can usually be inferred without ambiguity. In addition, these experiments provide no direct structural information about the ionic products. However, straightforward thermochemical arguments can often distinguish possibilities for isomeric structures.

Results and Discussion

Reaction of Fe⁺ and Ni⁺ with Methane. Only endothermic processes are observed in the interactions of iron and nickel ions with methane. The major product ion is MH^+ , while much smaller amounts of MCH_2^+ and MCH_3^+ are also formed. The latter two products account for <12% of the total product distribution in the Ni⁺ system and <7% in the Fe⁺ system. A possible mechanism for these reactions is shown in Scheme I. Oxidative addition of a C-H bond of methane to the metal forms 1 which may either rearrange via an α -hydrogen migration forming 2 or decompose directly by simple bond cleavage to give the ionic products MH^+ and MCH_3^+ . The enthalpies of reaction listed in Scheme I use bond energies to the metal listed in Table I.¹⁹ Because the $\text{M}^+ - \text{CH}_3$ bond is stronger than the $\text{M}^+ - \text{H}$ bond for both metal ions (see Table I), the former product is thermodynamically preferred. However, MH^+ is the predominant product at all energies examined, suggesting MH^+ is formed by a direct hydrogen abstraction process rather than via formation of an intermediate such as 1 which can fragment competitively. While reductive

(18) Levine, R. D.; Bernstein, R. B. "Molecular Reaction Dynamics"; Oxford: New York, 1974; p 42.

(19) Table I also uses $\Delta H_f(\text{CH}_4) = -17.89$ kcal/mol and $\Delta H_f(\text{H}) = 52.09$ kcal/mol from: Stull, D. R.; Prophet, H. *Natl. Stand. Ref. Data Ser. (U.S., Natl. Bur. Stand.)* 1971, 37. $\Delta H_f(\text{CH}_2) = 92.4$ kcal/mol from: Chase, M. W.; Curnutt, J. L.; Prophet, H.; McDonald, R. A.; Syverud, A. N. *J. Phys. Chem. Ref. Data, Suppl.* 1975, 4, No. 1. $\Delta H_f(\text{CH}_3) = 34.9$ kcal/mol from: Baghal-Vayjooee, M. H.; Colussi, A. J.; Benson, S. W. *J. Am. Chem. Soc.* 1978, 100, 3214.

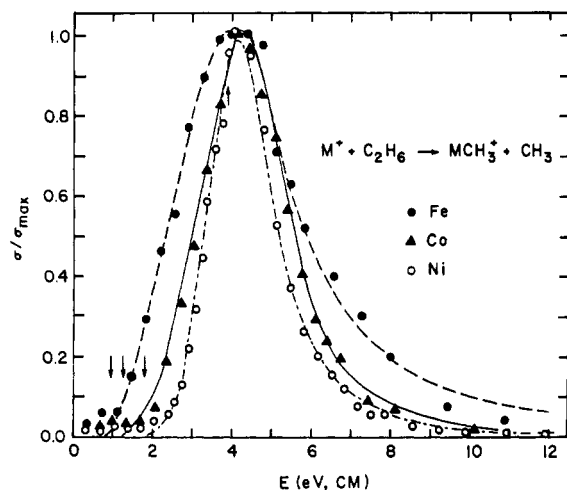
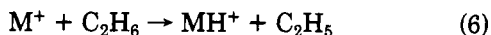
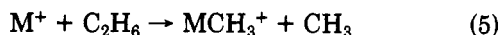


Figure 1. Variation in reaction cross section with kinetic energy in the center of mass frame for the formation of MCH_3^+ from reaction of M^+ with ethane, where $\text{M} = \text{Fe}, \text{Co},$ and Ni . For each system, the experimental cross section, σ , has been divided by the maximum cross section, σ_{max} . Arrows indicate the threshold energies at 0.91 eV (Fe), 1.25 eV (Co), and 1.8 eV (Ni) and the carbon-carbon bond energy of ethane, 3.9 eV.

elimination of a hydrogen molecule from 2 yielding MCH_2^+ is the least endothermic of the reactions observed, it involves the most extensive rearrangement.

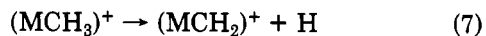
Reaction of Fe^+ and Ni^+ with Ethane. Both iron and nickel ions react with ethane in endothermic processes to give MCH_3^+ and MH^+ , reactions 5 and 6. Small amounts



of NiCH_2^+ , NC_2H_4^+ , and C_2H_5^+ are also detected at higher energies. Similar products were not observed in the Fe^+ -ethane system, indicating that cross sections for these reactions are less than 0.03 \AA^2 at all energies.

Detailed results for formation of the NiCH_3^+ and FeCH_3^+ ions are shown in Figure 1. The data are fit by using eq 4 and the parameters $n = 5$, $\sigma_0 = 44 \text{ \AA}^2$, $E_0 = 1.8 \text{ eV}$, and $a = 0.87$ for Ni^+ and $n = 3$, $\sigma_0 = 1.52 \text{ \AA}^2$, $E_0 = 0.91 \text{ eV}$, and $a = 0.85$ for Fe^+ .²⁰ Combining the threshold energies, E_0 , with the bond energy of ethane, 3.9 eV, we determine $D^0(\text{Ni}^+-\text{CH}_3) = 2.1 \pm 0.2 \text{ eV}$ ($48 \pm 5 \text{ kcal/mol}$) and $D^0(\text{Fe}^+-\text{CH}_3) = 3.0 \pm 0.2 \text{ eV}$ ($69 \pm 5 \text{ kcal/mol}$). These results are consistent with limits obtained by Ridge and Allison in an ion cyclotron resonance study of the reactions of atomic metal ions with methyl halides.^{6b} Their data give $56 \text{ kcal/mol} < D^0(\text{Fe}^+-\text{CH}_3) < 69 \text{ kcal/mol}$ and $D^0(\text{Ni}^+-\text{CH}_3) < 56 \text{ kcal/mol}$.

It is possible that the species having the formula $(\text{MCH}_3)^+$ has one or more hydrogens attached to the metal rather than corresponding to a metal methyl ion. However, calculations as in I indicate that ΔH_{rxn} for process 7 is in



(20) The data for the reactions of both Co^+ and Ni^+ with ethane to produce MCH_3^+ are fit with $n = 5$. It is unclear why a value of $n = 3$ gives a much better fit to the FeCH_3^+ data than $n = 5$. If $n = 5$ is used, a value of $E_0 = 0.6 \text{ eV}$ is obtained which results in $D^0(\text{Fe}^+-\text{CH}_3) = 3.3 \text{ eV}$ (76 kcal/mol). In this case, $\sigma_0 = 1.8 \text{ \AA}^2$. The procedure for fitting the model cross sections to the experimental data is such that the value of σ_0 scales in a highly nonlinear fashion with E_0 . For example, even though σ_{max} for the FeCH_3^+ system is only one-third that of the Co^+ or Ni^+ systems, the value for σ_0 is 25–30 times smaller for FeCH_3^+ ($n = 3$ –5) than for NiCH_3^+ . Because of this, one should not attach a great deal of physical significance to the geometrical parameter σ_0 . We also examined a more flexible threshold function, using a third-order polynomial to fit the experimental data. The threshold values obtained from this procedure are all within 0.33 eV of the quoted values (from the polynomial fits $E_0 = 0.6 \text{ eV}$, FeCH_3^+ ; 1.4 eV, CoCH_3^+ ; 2.1 eV NiCH_3^+).

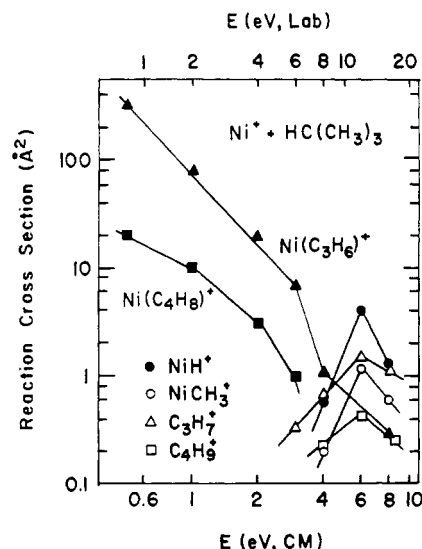


Figure 2. Variation in experimental cross section for the interaction of Ni^+ with 2-methylpropane as a function of kinetic energy in the center of mass frame (lower scale) and laboratory frame (upper scale).

the range of 70–85 kcal/mol.²¹ Since it seems more likely that a bond energy of this value represents a C–H bond weakened by resonance stabilization of the MCH_2^+ product rather than a metal–hydrogen bond,²² we conclude the structure involved is indeed a metal–methyl ion.

Figure 1 also includes the data for cobalt ions reacting with ethane to form CoCH_3^+ . In this figure, the experimental cross sections for each system have been normalized to 1.0 at their peaks. Maximum cross sections are of similar magnitudes: $\sigma_{\text{max}}(\text{Fe}^+) = 0.7 \text{ \AA}^2$, $\sigma_{\text{max}}(\text{Ni}^+) = 2.1 \text{ \AA}^2$, and $\sigma_{\text{max}}(\text{Co}^+) = 2.1 \text{ \AA}^2$. Several features of these reactions are worth noting. For example, data for all three systems peak approximately at the carbon-carbon bond dissociation energy of ethane, 3.9 eV. A cursory inspection of Figure 1 reveals the relative metal ion–methyl bond strengths. Iron ions have the lowest threshold, and therefore the largest bond energy, followed by Co^+ and then Ni^+ . The larger bond energy is also consistent with a slower decrease in cross section with increasing energy for the FeCH_3^+ product at high energy, which suggests that a higher internal energy is required for this species to fragment.

Table I lists the bond dissociation energies $D^0(\text{M}^+-\text{X})$ where $\text{M} = \text{Fe}, \text{Co},$ and Ni and $\text{X} = \text{H}, \text{CH}_3,$ and CH_2 . In a recent communication,¹¹ we noted that the metal ion hydride and methyl bond energies for Cr, Mn, Fe, Co, Ni, and Zn correlate with the energy required to promote the metal ion from its ground state to the lowest state derived from the $(3d)^{n-1}(4s)$ configuration.²³ The implication of this result is that σ bonding to the first-row transition metals involves substantial participation of the metal 4s orbital, as is predicted by several theoretical calculations.^{9,24} This explains why iron ions, whose ground state is a favored bonding configuration, $(3d)^6(4s)$, make strong bonds

(21) ΔH_{rxn} of process 7 can be calculated by using only the endothermicities of the reactions forming $(\text{MCH}_3)^+$ and $(\text{MCH}_2)^+$, with no prior assumptions about the structure of the ions. For Fe^+ , $\Delta H_{\text{rxn}} = 83 \text{ kcal/mol}$, while for Ni^+ , $\Delta H_{\text{rxn}} = 72 \text{ kcal/mol}$.

(22) From other studies we have determined $D^0(\text{Fe}^+-\text{H}) = 58 \pm 5 \text{ kcal/mol}$ ¹¹ and $D^0(\text{Ni}^+-\text{H}) = 43 \pm 2 \text{ kcal/mol}$.^{10b}

(23) No such correlation is found for $D^0(\text{M}^+-\text{CH}_2)$, presumably the result of variable amounts of π bonding in this system.

(24) Scott, P. R.; Richards, W. G. "The Electronic Structure of Diatomic Transition Metal Molecules", *Chem Soc. Spec. Period. Rep.* 1976, 4, 70.

Table II. Product Distributions of Exothermic Reactions of Fe⁺, Co⁺, and Ni⁺ with Alkanes Measured at ~1-eV Relative Kinetic Energy

| reactant alkane | structure | M ⁺ | neutral products (C _m H _{2m+2}) corresponding to ionic product M(C _{n-m} H _{2(n-m)}) ⁺ | | | | | | neutral products corresponding to M(alkadiene) ⁺ products | | | | |
|--------------------------------|---------------------------|----------------|---|-----------------|-------------------------------|-------------------------------|--------------------------------|--------------------------------|--|----------------------------------|--|--|------|
| | | | H ₂ | CH ₄ | C ₂ H ₆ | C ₃ H ₈ | C ₄ H ₁₀ | C ₅ H ₁₂ | 2H ₂ | H ₂ + CH ₄ | H ₂ + C ₂ H ₆ | H ₂ + C ₃ H ₈ + CH ₄ + C ₂ H ₆ | |
| C ₃ H ₈ | propane | Fe | 0.44 | 0.56 | | | | | | | | | |
| | | Co | 0.59 | 0.41 | | | | | | | | | |
| | | Ni | 0.20 | 0.80 | | | | | | | | | |
| C ₄ H ₁₀ | butane | Fe | 0.27 | 0.36 | 0.28 | | | | 0.07 | | | | |
| | | Co | 0.29 | 0.12 | 0.59 | | | | | | | | |
| | | Ni | 0.24 | 0.17 | 0.59 | | | | | | | | |
| | 2-methylpropane | Fe | 0.54 | 0.46 | | | | | | | | | |
| | | Co | 0.23 | 0.77 | | | | | | | | | |
| | | Ni | 0.11 | 0.89 | | | | | | | | | |
| C ₅ H ₁₂ | pentane | Fe | 0.16 | 0.18 | 0.27 | 0.22 | | | | 0.16 | | | |
| | | Co | 0.30 | 0.02 | 0.59 | 0.08 | | | | | | | |
| | | Ni | 0.29 | 0.04 | 0.49 | 0.16 | | | | | 0.02 | | |
| | 2-methylbutane | Fe | 0.24 | 0.27 | 0.20 | 0.04 | | | | 0.03 | 0.22 | | |
| | | Co | 0.20 | 0.37 | 0.27 | 0.05 | | | | 0.02 | 0.05 | | |
| | | Ni | 0.13 | 0.27 | 0.40 | 0.13 | | | | | 0.07 | | |
| | 2,2-dimethylpropane | Fe | | 1.0 | | | | | | | | | |
| | | Co | | 1.0 | | | | | | | | | |
| | | Ni | | 1.0 | | | | | | | | | |
| C ₆ H ₁₄ | hexane | Fe | 0.20 | 0.10 | 0.18 | 0.23 | 0.23 | | | | | 0.06 | |
| | | Co | 0.39 | 0.02 | 0.35 | 0.16 | 0.04 | | | | | 0.05 | |
| | | Ni | 0.48 | | 0.27 | 0.17 | 0.05 | | | | | 0.03 | |
| | 2,2-dimethylbutane | Fe | 0.03 | 0.08 | 0.62 | 0.06 | 0.04 | | | | 0.06 | 0.10 | |
| | | Co | 0.12 | 0.30 | 0.40 | 0.03 | 0.02 | | | | 0.05 | 0.07 | |
| | | Ni | 0.05 | 0.17 | 0.54 | 0.03 | 0.06 | | | | 0.06 | 0.09 | |
| | 2,3-dimethylbutane | Fe | 0.05 | 0.06 | 0.07 | 0.13 | 0.01 | | | 0.08 | 0.38 | 0.22 | |
| | | Co | 0.22 | 0.35 | | 0.23 | | | | | 0.09 | 0.11 | |
| | | Ni | 0.10 | 0.16 | 0.02 | 0.61 | 0.02 | | | | 0.03 | 0.06 | |
| C ₇ H ₁₆ | heptane | Fe | 0.18 | 0.04 | 0.11 | 0.26 | 0.20 | 0.18 | | | | | 0.02 |
| | | Co | 0.28 | 0.01 | 0.15 | 0.22 | 0.28 | 0.04 | | | | | 0.02 |
| | | Ni | 0.33 | | 0.14 | 0.22 | 0.21 | 0.09 | | | | | 0.01 |
| C ₈ H ₁₈ | 2,2,3,3-tetramethylbutane | Fe | 0.02 | 0.08 | | 0.05 | 0.08 | | | | | 0.71 | 0.06 |
| | | Co | 0.07 | 0.16 | | 0.05 | 0.13 | | | | 0.03 | 0.55 | |
| | | Ni | 0.04 | 0.18 | | 0.04 | 0.26 | | | | 0.02 | 0.42 | |

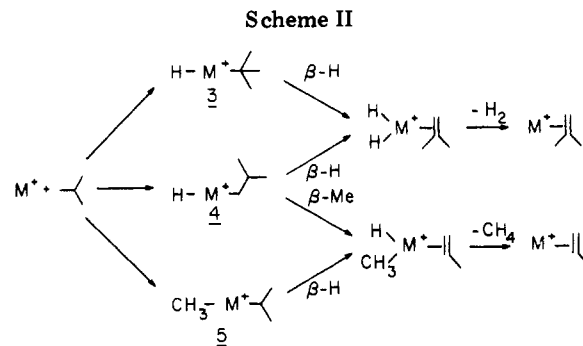
to H and CH₃ radicals. These same bonds to nickel ions, which require 24 kcal/mol to be promoted from their ground state into the (3d)⁸(4s) configuration,¹³ are much weaker. Cobalt ions require 9.6 kcal/mol to be promoted into the (3d)⁷(4s) configuration.¹³ Accordingly, *D*⁰(Co⁺-H) and *D*⁰(Co⁺-CH₃) have values intermediate to those of Fe⁺ and Ni⁺.

Reactions of Fe⁺ and Ni⁺ with Larger Alkanes. Table II lists the results for exothermic reactions of Fe⁺ and Ni⁺ with several alkanes. Ionic products seen at low energies all have the molecular formula M(C_nH_{2n})⁺. From the stoichiometry and thermochemistry of the reactions, neutral products are inferred to be the corresponding alkanes or a hydrogen molecule. At the lowest energies examined, the metal-alkane adduct is also seen. Pressure dependence studies indicate that this product is formed in a termolecular process.

Figure 2 shows data for reaction of Ni⁺ with 2-methylpropane as an example. At low energies the reaction cross sections for formation of Ni(C₃H₈)⁺ and Ni(C₄H₈)⁺ are large and decrease with increasing energy, indicating that processes 8 and 9 are exothermic. At higher energies,



products of endothermic reactions appear. In the reaction of Ni⁺ with 2-methylpropane these include, most prominently, NiH⁺, NiCH₃⁺, C₃H₇⁺, and C₄H₉⁺. (Figure 2). For the other alkanes examined, the metal hydride and metal

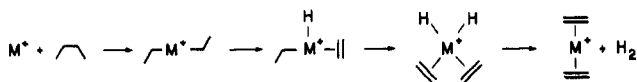


alkyl as well as the corresponding alkyl ions are also observed at the higher energies with both metal ions. The product distributions given in Table II agree fairly well with ICR studies of Allison and Ridge^{6a,c} for reactions of Fe⁺, Co⁺, and Ni⁺ with butanes and of Byrd, Burnier, and Freiser²⁵ for reactions of Fe⁺ with several alkanes, though the latter study does not report any Fe(alkadiene)⁺ products.

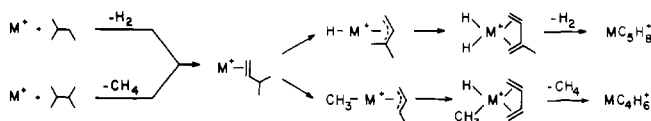
The reactions of Fe⁺ and Ni⁺ with larger alkanes yield products analogous to those observed from the corresponding reactions of Co⁺.¹² Similar reactivities and product distributions listed in Table II suggest that the three metal ions react via the same mechanism. Scheme II depicts the proposed reaction mechanism in the case of

(25) Byrd, G. D.; Burnier, R. C.; Freiser, B. S. *J. Am. Chem. Soc.*, submitted for publication.

Scheme III



Scheme IV



2-methylpropane. Oxidative addition of the three types of bonds available to the metal center is followed by β -hydrogen or β -methyl transfer to the metal and reductive elimination of an alkane or H_2 yielding a metal ion-alkene complex. Evidence for this mechanism is the same as that derived from reactions of Co^+ with these and other alkanes.¹² Dehydrogenation of alkanes can also occur via insertion into internal C-C bonds followed by two β -hydrogen transfers (Scheme III). Nickel ions appear to dehydrogenate linear alkanes larger than propane exclusively via this latter mechanism.²⁶ Results with Fe^+ and Co^+ suggest a more complex process in which reversible β -hydrogen transfers may obscure the actual mechanism.¹²

The products shown in Schemes II and III are alkenes bound to the metal ion. Binding energies of group 8 metal ions to ethene are in the range of 30–60 kcal/mol.²⁷ Hence it is the stability of the products which renders the overall process substantially exothermic when effected by a transition-metal ion. If sufficient energy is retained by the metal-alkene complex, further reaction may occur to yield a metal ion-alkadiene complex (Scheme IV). This process begins by insertion of the metal ion into an allylic C-C or C-H bond followed by either a simple β -H transfer or by more complicated isomerization and cleavage reactions.²⁹ The metal then reductively eliminates H_2 , an alkane, or an alkene. These reactions explain the occurrence of some products which are not accounted for by the general mechanism outlined in the previous study with Co^+ .¹² For example, in the case of M^+ reacting with 2,3-dimethylbutane, the further reaction of $M(2,3\text{-dimethyl-2-butene})^+$ can account for the loss of $2H_2$, $H_2 + CH_4$, and $H_2 + C_2H_6$ as well as C_2H_6 ($H_2 + C_2H_4$) and C_4H_{10} ($H_2 + C_4H_8$).²⁹ Note that two of these products, those corresponding to loss of $2H_2$ and C_2H_6 , could not arise from further reaction of $M(3\text{-methyl-1-butene})^+$. However, the latter ion is probably formed as well and may account for the large amount of $M(C_4H_8)^+$ product in the reaction of Fe^+ with 2,3-dimethylbutane.

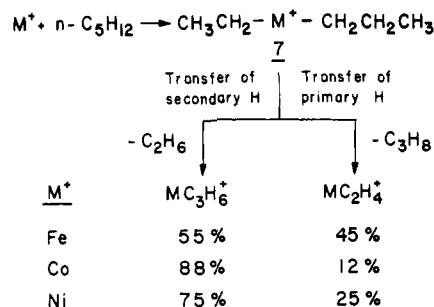
(26) Halle, L. F.; Houriet, R.; Kappes, M. M.; Staley, R. H.; Beauchamp, J. L., submitted for publication in *J. Am. Chem. Soc.*

(27) If the failure of M^+ to dehydrogenate ethane at low ion energies is a result of the overall process being endothermic, then $D^0(M^+-C_2H_4) < 33$ kcal/mol.²⁸ However, reactions of Co^+ with alkenes²⁹ indicate that the binding energies of both ethene and propene exceed 36 kcal/mol. The lower limit of 36 kcal/mol is the more reliable value, but it seems likely that the binding energy of C_2H_4 to Co^+ cannot exceed this limit greatly. ICR experiments have shown that C_2D_4 can displace CO from $FeCO^+$: Foster, M. S.; Beauchamp, J. L. *J. Am. Chem. Soc.* 1975, 97, 4808, while photoionization studies have determined $D^0(Fe^+-CO) = 2.62 \pm 0.1$ eV (60.5 ± 2 kcal/mol): Distefano, G. *J. Res. Natl. Bur. Stand., Sect. A* 1970, 74A, 233. This latter value may be too high, however. The threshold for $FeCO^+$ formation appears closer to 12.40 eV rather than 11.53 eV as suggested by Distefano. This lowers $D^0(Fe^+-CO)$ to 1.63 eV (37.6 kcal/mol).

(28) Supplementary heats of formation of hydrocarbons are taken from: Cox, J. D.; Pilcher, G. "Thermochemistry of Organic and Organometallic Compounds"; Academic Press: New York, 1970.

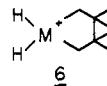
(29) Armentrout, P. B.; Halle, L. F.; Beauchamp, J. L. *J. Am. Chem. Soc.* 1981, 103, 6624.

Scheme V



Scheme II also accounts for products observed at higher energies. In the example of 2-methylpropane, decomposition of intermediates 3, 4, and 5 can occur by simple bond cleavage not accessible at thermal energies. Since these processes often have favorable frequency factors, they become the dominant decomposition route at the higher energies. Here intermediates 3 and 4 yield MH^+ and $C_4H_9^+$, while 5 gives MCH_3^+ and $C_3H_7^+$. In the case of Ni^+ , where insertion into C-H bonds is less important,²⁶ the NiH^+ may be mainly the result of a high-energy stripping process.

The only products which cannot be accounted for by the pathways described above occur in the reactions of all three ions with 2,2,3,3-tetramethylbutane. As suggested in I, the dehydrogenation of this compound could be due to the formation of the metallacycle 6, or via a process analogous



to Scheme III. Further reaction of the ion formed by loss of methane, $M(C_7H_{14})^+$, probably accounts for the small amounts of $M(C_7H_{12})^+$, $M(C_5H_{10})^+$, and $M(C_5H_8)^+$ observed.

As examination of Table II does reveal some differences of reactivity between the metal ions which can be qualitatively explained in terms of energetics. The enthalpy change for the general process 10 is given in terms of the



$$\Delta H = D(R_1R_2) - D(MR_1^+-R_2) - D(M^+-R_1) \quad (11)$$

various bond dissociation energies by eq 11. Bond energy data for the species $MR_1R_2^+$ are not available. Hence we will assume bond additivity and approximate $D(MR_1^+-R_2)$ by $D(M^+-R_2)$. Using $D(C-H) = 95$ kcal/mol and $D(C-C) = 85$ kcal/mol as typical values for carbon-hydrogen and carbon-carbon bond dissociation energies permits several conclusions to be drawn from the data presented in Table I. Bond energies to iron are the strongest and the energetics suggest that insertion into both C-H and C-C bonds should be significantly exothermic and indiscriminate. These processes should be highly selective for nickel ions, while cobalt ions represent an intermediate case.

Consistent with the above considerations, iron ions are less selective in inserting into C-C bonds of alkanes. In I, it was noted that initial oxidative addition occurs preferentially with the weakest bonds of the alkane. This is true for both Co^+ and Ni^+ , as can be seen from the less frequent production of methane, resulting from M^+ inserting into terminal C-C bonds, than products from reactions involving insertion into internal C-C bonds. However, insertion into the stronger terminal C-C bond is much more prevalent for Fe^+ reactions, as indicated by the higher proportions of loss of CH_4 , $H_2 + CH_4$, and $2CH_4$. The $M(\text{alkadiene})^+$ products probably arise from $M(\text{al-$

kene)⁺ complexes which are formed by both initial loss of H₂ and initial loss of CH₄ (Scheme IV).

Another feature of the reaction of Co⁺ with alkanes noted in I is that transfer of secondary β -hydrogens in reaction intermediates is more likely than primary β -hydrogen transfers.¹² For example, in the reaction with *n*-pentane, intermediate 7 which results from initial insertion into an internal C-C bond can either transfer a secondary β -hydrogen and eliminate ethane or transfer a primary β -hydrogen and lose propane (Scheme V). The product distributions listed in Scheme V show that in reactions with Ni⁺ as well as Co⁺ a secondary β -hydrogen transfer is greatly favored. However, reactions of Fe⁺ with *n*-pentane and other alkanes deviate somewhat from this pattern. This may be due to the higher internal energy of 7 caused by the greater exothermicity of the initial insertion of Fe⁺ into the C-C bond.

The M(alkene)⁺ products may retain part of the exothermicity of the initial insertion reaction as internal excitation. Because the insertion process is most exothermic for Fe⁺, one expects the Fe(alkene)⁺ product to have more energy to further react than the corresponding products of Co⁺ and Ni⁺. Consistent with this observation are the higher proportions of M(alkadiene)⁺ products of reactions of Fe⁺ with alkanes relative to reaction of Co⁺ and Ni⁺.

Periodic Trends in Metal Ion Reactivity. The group 8 metal ions Fe⁺, Co⁺, and Ni⁺ exhibit very similar reactivity with alkanes. Subtle differences are rationalized as being mainly due to differences in reaction thermochemistry. We have also examined the reactions of Mn⁺ and Cr⁺ with alkanes.³⁰ In comparison to the group 8

metals, these species are quite unreactive, and processes such as dehydrogenation and carbon-carbon bond cleavage are not observed. In part, this is due to weaker metal-hydrogen and metal-carbon bond dissociation energies for these elements. The possible relationship of these results to the electronic structures of the organometallic fragments is discussed elsewhere.¹¹ To compare with Co⁺, we have also briefly examined the reaction of Rh⁺³¹ (which in analogy with Co⁺ has a ³F ground state derived from the d⁸ configuration). Unlike Co⁺, Rh⁺ does not readily cleave carbon-carbon bonds and instead is observed mainly to dehydrogenate hydrocarbons. With these limited results, it is obviously difficult to offer many generalizations concerning periodic trends in reactivity and thermochemical properties. Studies of a wider range of atomic metal ions and clusters are currently in progress. In addition, we are developing sources of metal atoms which will permit related chemistry of the neutral species to be explored.

Acknowledgment. We wish to thank Dr. Raymond Houriet for his contributions to this paper and to Mr. Arthur Voter and Dr. Arthur S. Gaylord for their help in providing computer programs used in fitting the data. This research was supported in part by the U.S. Department of Energy. Graduate fellowship support from Bell Laboratories (L.F.H.) is gratefully acknowledged.

Registry No. Fe⁺, 14067-02-8; Co⁺, 16610-75-6; Ni⁺, 14903-34-5; propane, 74-98-6; butane, 106-97-8; 2-methylpropane, 75-28-5; pentane, 109-66-0; 2-methylbutane, 78-78-4; 2,2-dimethylpropane, 463-82-]; hexane, 110-54-3; 2,2-dimethylbutane, 75-83-2; 2,3-dimethylbutane, 79-29-8; heptane, 142-82-5; 2,2,3,3-tetramethylbutane, 594-82-1.

(30) Halle, L. F.; Armentrout, P. B.; Beauchamp, J. L., unpublished data.

(31) Beauchamp, J. L., unpublished data.

Conformational Variability in Tricarbonyl(hexaethylborazine)chromium(0)

Geoffrey Hunter,*^{1a} William S. Wadsworth, Jr.,^{1b,c} and Kurt Mislow*^{1c}

Departments of Chemistry, The University, Dundee DD1 4HN, Scotland, and Princeton University, Princeton, Princeton, New Jersey 08544

Received January 29, 1982

Evidence is adduced from variable-temperature ¹³C NMR studies for the presence of two conformers in CD₂Cl₂ solutions of the title compound. Line-shape analyses are consistent with the assignment of C_s symmetry to both conformers. In one of these, two terminal methyl groups on N-Et are proximal to the metal atom, while in the other only one such group is proximal. Interconversion of the conformers requires a barrier of $\Delta G^\ddagger = 10.4$ kcal mol⁻¹. The conformational variability in this system parallels similar findings for hexaethylbenzene transition metal π complexes.

Recent structural studies of hexaethylbenzene (HEB) transition metal π complexes of the type (HEB)·ML₃ (1)² have provided evidence of a marked preference for the four conformational types shown in Figure 1 (top and bottom rows). Examples of three types are known:² 1a ((HEB)-

Cr(CO)₃, (HEB)Mo(CO)₃), 1e ((HEB)Cr(CO)₂PEt₃), and 1h ((HEB)Cr(CO)₂PEt₃, (HEB)Cr(CO)₂PPh₃). Although no representative of the missing type 1c has yet been reported, a formal analogy may be drawn between 1c and 2c (Figure 1, middle row), the conformation found in the crystal of tricarbonyl(hexaethylborazine)chromium(0) (2).³ In this compound, which also has the distinction of being the only borazine transition metal complex with a known

(1) (a) University of Dundee. (b) On leave from South Dakota State University, 1980. (c) Princeton University.

(2) Iverson, D. J.; Hunter, G.; Blount, J. F.; Damewood, J. R., Jr.; Mislow, K. *J. Am. Chem. Soc.* 1981, 103, 6073. Hunter, G.; Blount, J. F.; Damewood, J. R., Jr.; Iverson, D. J.; Mislow, K. *Organometallics* 1982, 1, 448.

(3) Huttner, G.; Krieg, B. *Angew. Chem., Int. Ed. Engl.* 1971, 10, 512; *Chem. Ber.* 1972, 105, 3437.